"Optimal" approximation and the realistic nucleon-nucleon interactions

J. L. Ballot
Division de Physique Théorique, Institut de Physique Nucléaire, F-91406 Orsay Cedex, France

L. Leśniak
Institute of Nuclear Physics, PL-31-342 Kraków, Poland
(Received 18 April 1988)

The "optimal" approximation in the presence of the realistic nucleon-nucleon forces is tested for the proton-deuteron elastic scattering in the laboratory kinetic energy range between 100 and 450 MeV. The particular emphasis is put on the large scattering angles where the corrections to the *pd* scattering amplitude are governed by the energy derivative of the off-shell nucleon-nucleon amplitudes. At 180° the second-order relative corrections amount to 10 or 20 % in the energy range up to 320 MeV and are much larger at higher energies, especially at about 400 MeV—the energy corresponding to the zero of the scalar deuteron form factor. In the forward direction the corrections are very small: 1 to 5 %. Their maximum values are found for the proton-bound neutron scattering at the intermediate angles close to 90°.

I. INTRODUCTION

The principal aim of introducing the so-called "optimal" approximation[1,2] for the projectile-nucleus elastic scattering is to take into account the binding and recoil effects at the relatively large momentum transfers where the impulse or Glauber approximations break down. The accuracy of this approximation has been studied[3] for the proton-deuteron elastic scattering at intermediate energies using the local nucleon-nucleon interactions independent of the target nucleon spin. The deuterium target has been chosen because the deuteron wave function is sufficiently well known for the large relative proton-neutron momenta. The direct studies of the three-nucleon scattering at the incoming nucleon energies of several hundred MeV are in progress for the modern nucleon-nucleon forces although they have been done at rather low energies of 10 and 20 MeV.[4] At higher energies we still have to use some approximate schemes to describe the complex nucleon-nucleus interactions.

In previous studies of the "optimal" approximation the nucleon-nucleon scattering matrix has often been parametrized as a single Gaussian function of the momentum transfer. Obviously, in this case no spin dependence has been included. In this paper we use the *realistic spin-dependent* nucleon-nucleon potentials to calculate the scattering amplitudes. We restrict ourselves to the proton laboratory kinetic energies lower than 450 MeV where the nucleon potentials reproduce well the two-nucleon scattering data as well as the properties of the deuteron bound state.

In the "optimal" approximation the nucleon-deuteron single scattering amplitude is proportional to the *on-shell* nucleon-nucleon amplitude calculated at the *effective* energy $E_{\rm ef}$ growing with the increasing momentum transfer. To study the corrections to this amplitude we also need the *off-energy-shell* amplitudes which have been, and are currently studied in relation to many-particle calculations.[5–7] As we shall see, the largest correction to the backward *pd* scattering amplitude is proportional to the *energy derivative* of the off-shell nucleon-nucleon scattering amplitude. In Ref. 1, this derivative has been estimated to vary as an inverse power of energy like it has been done by Goldberger and Watson in the study of corrections to the impulse approximation.[8] Next, in Ref. 3, a more general parametrization with one free parameter has been introduced. In the present article we can verify the preceding estimations by separately calculating the off-shell nucleon-nucleon amplitudes and their derivatives. The result is that the energy variation of the amplitudes for the scattering angles close to 0° or 180° is weaker than the estimated inverse power behavior. In the calculations we apply the method developed in Ref. 5. Three different potentials are used: The Reid soft-core potential[9] (RSC) modified by Day[10] for the potential waves higher than 2, the super-soft-core *C* potential[11] (SSCC), and the Argonne V_{14} potential.[12] The full range of the scattering angles is covered with a particular emphasis on the backward hemisphere.

The analysis of the realistic nucleon-nucleon amplitudes is the first subject of the paper. The second one is its application to the study of corrections to the "optimal" approximation for the proton scattering on a single nucleon *bound* in deuteron. Here, we take fully into account the spin dependence of the amplitudes. This part of our work could constitute the first attempt towards a much more complicated analysis of the multiple-scattering terms in the same approximation. So, at present, our aim is not to test the results against the experimental proton-deuteron data. We should mention, however, the fact that both the proton-proton and proton-neutron amplitudes averaged over the nucleons spin projections rise at the backward scattering angles. This means that the modulus of the single nucleon-deuteron scattering amplitude also has the backward maximum. It is therefore very likely that the backward

pd elastic amplitude is dominated by the single scattering term (compare Ref. 13). If that is the case, then we can expect that the magnitude of the corrections to the full amplitude in the backward direction remains the same after inclusion of other scattering terms. On the other hand, for the small scattering angles we know that the single scattering amplitude is the most important one and the present approach gives us the information about the binding and recoil corrections to it.

In Sec. II we derive the new formulae for the "optimal" amplitude in the presence of the spin-dependent forces and examine its first-order correction. Section III deals with the most important second-order correction. In Sec. IV the dependence of the nucleon-nucleon scattering amplitudes and their derivatives as functions of the energy and the scattering angle are presented. In Sec. V we analyze the numerical results of the corrections and in Sec. VI we give the concluding remarks.

II. "OPTIMAL" AMPLITUDE AND THE FIRST-ORDER CORRECTION

In this paper we examine the first- and second-order corrections δ_1 and δ_2 to the scattering matrix T_1 corresponding to the elastic projectile scattering on one of the two nucleons bound in deuteron (we follow the notation of Ref. 3). This matrix T_1 gives the "optimal" scattering operator for the transition from the initial state $|\mathbf{p},\kappa,\lambda\rangle$ to the final state $|\mathbf{p}',\kappa',\lambda'\rangle$, where $\mathbf{p}$ and $\mathbf{p}'$ are the initial and final projectile momenta, κ and κ' are the projectile spin projections, and λ and λ' are the deuteron spin projections. Let us take the proton as the incident particle, so the scattering matrix T_1 has $6\times6=36$ elements. These 36 elements can be expressed in terms of the 12 independent proton-deuteron amplitudes.[14] For the further discussion we choose from these 36 elements a scalar amplitude T_s which is given by the average over all the spin projections in the both initial and final states

$$T_s(\mathbf{p}',\mathbf{p},E_{\rm ef})=\tfrac{1}{6}\sum_{\kappa\lambda}\langle\mathbf{p}',\kappa,\lambda\,|\,T_1\,|\,\mathbf{p},\kappa,\lambda\rangle\ . \tag{1}$$

The amplitude T_s which is also a function of the effective energy $E_{\rm ef}$ can be expressed in the factorized form

$$T_s(\mathbf{p}',\mathbf{p},E_{\rm ef})=t_s(\mathbf{p}',\mathbf{p},E_{\rm ef})\phi_S(\mathbf{q})\ , \tag{2}$$

where t_s is the spin averaged *on-shell* proton-nucleon amplitude

$$t_s(\mathbf{p}',\mathbf{p},E_{\rm ef})=\tfrac{1}{4}\sum_{\kappa\eta}\langle\mathbf{p}',\kappa,\eta\,|\,t\,|\,\mathbf{p},\kappa,\eta\rangle\ , \tag{3}$$

$\phi_S(q)$ is the scalar deuteron form factor and $\mathbf{q}=\mathbf{p}-\mathbf{p}'$ is the momentum transfer. In the preceding equation η denotes the target nucleon spin projection and t_s is the proton-target nucleon scattering matrix. The amplitude t_s is sometimes called a spin-independent nucleon-nucleon amplitude because it constitutes the first term of the amplitude expansion in the two-dimensional spin operators space of individual nucleons.[15]

Let us discuss the first correction δ_1 to the "optimal" amplitude (2) which is also averaged over the nucleon and deuteron spin projections as in (1):

$$\delta_1=\tfrac{1}{6}\sum_{\kappa\lambda}\langle\mathbf{p}',\kappa,\lambda\,|\,t_aG_ahG_at_a\,|\,\mathbf{p},\kappa,\lambda\rangle\ . \tag{4}$$

In this equation t_a is an approximated ("optimal") proton-nucleon amplitude and the operator $h=G_a^{-1}-G^{-1}$, where G_a and G are the approximated and the full Green's functions (see Ref. 3 for definitions). The second Green's function depends on the deuteron Hamiltonian H which in turn contains the proton-neutron interaction V_{pn}. It depends on the both nucleon spin operators as t_a depends on the spin of the target nucleon. Let us suppose that the incident proton scatters on the target neutron. Then we can write

$$t_a=f+\mathbf{g}\cdot\boldsymbol{\sigma}_n\ , \tag{5}$$

where f and $\mathbf{g}$ can still depend on the incoming proton spin operator and $\boldsymbol{\sigma}_n$ is the target neutron Pauli spin operator. The interaction V_{pn} can be written as

$$V_{pn}=V+\mathbf{W}\cdot\boldsymbol{\sigma}_n\ , \tag{6}$$

and we admit that V and $\mathbf{W}$ can further depend on the *target* proton spin operator. As previously indicated, we use the Schrödinger equation when the operator h acts directly on the deuteron initial state in $|\mathbf{p},\nu,\mu\rangle$ [Eq. (4)]. The commutator $[h,G_a]=0$ as for the spin independent forces but the second commutator

$$[h,t_a]=[V_{pn},t_a]=2i(\mathbf{W}\times\mathbf{g})\cdot\boldsymbol{\sigma}_n \tag{7}$$

does not vanish in general. It has the particular feature that the two neutron spin-flip operators $\mathbf{W}$ and $\mathbf{g}$ act together. Moreover, we still have to perform the summation over all the spin projections after the multiplication by the other t_a operator standing on the left-hand side of h in (4). It can be seen that many terms vanish and we therefore neglect the remaining contribution of this at least double target neutron spin-flip term. Once this is done, the operator form of the correction $\hat{\delta}_1$ in the spin space can be written exactly in the same way as in Ref. 3

$$\hat{\delta}_1=\int d^3Qd^3k_1\psi^\dagger(\mathbf{Q}+\tfrac{1}{4}\mathbf{q})\frac{\langle\mathbf{k}'\,|\,t\,|\,\mathbf{k}_1\rangle\langle\mathbf{k}_1\,|\,t\,|\,\mathbf{k}\rangle}{(E_{\rm ef}-k_1^2/m)^2}\times\frac{(\mathbf{k}-\mathbf{k}_1)\cdot\mathbf{Q}}{m}\psi(\mathbf{Q}-\tfrac{1}{4}\mathbf{q})\ , \tag{8}$$

where ψ is the deuteron wave function and m is the nucleon mass. We should, however, remember that the incoming proton-target neutron *half-shell* amplitudes ($E_{\rm ef}=k^2/m=k'^2/m$)

$$t_1\equiv\langle\mathbf{k}'\,|\,t\,|\,\mathbf{k}_1\rangle=f_1+\mathbf{g}_1\cdot\boldsymbol{\sigma}_n\ , \tag{9}$$

$$t_2\equiv\langle\mathbf{k}_1\,|\,t\,|\,\mathbf{k}\rangle=f_2+\mathbf{g}_2\cdot\boldsymbol{\sigma}_n\ , \tag{10}$$

are the operators in the spin space of two interacting nucleons. The vectors $\mathbf{k}$, $\mathbf{k}'$, and $\mathbf{k}_1$ are the relative projectile-neutron momenta. The product t_1t_2 can be written as

$$t_1t_2=F+\mathbf{G}\cdot\boldsymbol{\sigma}_n\ , \tag{11}$$

where

$$F=f_1f_2+\mathbf{g}_1\cdot\mathbf{g}_2 \tag{12}$$

and

$$\mathbf{G}=f_1\mathbf{g}_2+f_2\mathbf{g}_1+i\mathbf{g}_1\times\mathbf{g}_2 \ . \tag{13}$$

In these equations we point out the dependence on the neutron spin operator σ_n since we shall further calculate the matrix elements between the deuteron wave functions. We stress, however, that all the operators f_1, f_2, $\mathbf{g}_1$, $\mathbf{g}_2$, F, and $\mathbf{G}$ also act in the incoming proton spin space. In the target neutron space, F can be written as a trace,

$$F=\tfrac{1}{2}\mathrm{tr}(t_1t_2) \tag{14}$$

and since we also need to average over the incoming proton spin projections, we introduce a symbol

$$\langle tt\rangle=\tfrac{1}{4}\mathrm{tr}(t_1t_2) \ , \tag{15}$$

where the trace is taken in *both* the proton and neutron spin spaces, as in (3).

The contribution to δ_1 proportional to F [in (11)] vanishes after the averaging over the deuteron spin projections [see (24) of Ref. 3]. For the second part $\mathbf{G}\cdot\sigma_n$ we expect some contribution coming from

$$S(\mathbf{q},\boldsymbol{\rho},\mathbf{G})=\int d^3Q\ \psi^\dagger(\mathbf{Q}+\tfrac{1}{4}\mathbf{q})\mathbf{Q}\cdot\boldsymbol{\rho}\mathbf{G}\cdot\sigma_n\psi(\mathbf{Q}-\tfrac{1}{4}\mathbf{q}) \ , \tag{16}$$

where $\boldsymbol{\rho}=\mathbf{k}-\mathbf{k}_1$. After some algebra we get the following expression for the scalar part of S (S averaged over the deuteron spin projection—a procedure equivalent to taking the trace in the deuteron spin space)

$$S_{\mathrm{scalar}}(\mathbf{q},\boldsymbol{\rho},\mathbf{G})=12i\int d^3Q\ \psi_d(\mathbf{p}_1)\mathbf{Q}\cdot\boldsymbol{\rho}\,\hat{\mathbf{p}}_1\cdot\hat{\mathbf{p}}_2(\hat{\mathbf{p}}_1\times\hat{\mathbf{p}}_2)\cdot\mathbf{G}\psi_d(\mathbf{p}_2) \ , \tag{17}$$

where

$$\mathbf{p}_1=\mathbf{Q}+\tfrac{1}{4}\mathbf{q}, \quad \mathbf{p}_2=\mathbf{Q}-\tfrac{1}{4}\mathbf{q} \ ,$$

$$\hat{\mathbf{p}}_1=\mathbf{p}_1/p_1, \quad \hat{\mathbf{p}}_2=\mathbf{p}_2/p_2 \ ,$$

and $\psi_d(p)$ is the *d state* part of the deuteron wave function. Because of the presence of two d-state wave functions we expect that its contribution is very small. In this manner we have *minimized* the first-order correction to the "optimal" amplitude T_s.

III. SECOND-ORDER CORRECTION

The second-order correction depends on the second power of the operator h appearing in (4):

$$\delta_2=\tfrac{1}{6}\sum_{\kappa\lambda}\langle\mathbf{p}',\kappa,\lambda\mid t_aG_ahG_ahG_at_a\mid\mathbf{p},\kappa,\lambda\rangle \ . \tag{18}$$

As in Sec. II we transpose h and t_a operators neglecting the multispin-flip terms of the target neutron. Then using the Schrödinger equation we find the expression

$$\hat{\delta}_2=\frac{1}{m^2}\int d^3k_1d^3Q\psi^\dagger(\mathbf{Q}+\tfrac{1}{4}\mathbf{q})\mathbf{Q}\cdot(\mathbf{k}'-\mathbf{k}_1)\frac{\langle tt\rangle}{(E_{\mathrm{ef}}-k_1^2/m)^2}\cdot\mathbf{Q}\cdot(\mathbf{k}-\mathbf{k}_1)\psi(\mathbf{Q}-\tfrac{1}{4}\mathbf{q}) \ , \tag{19}$$

where the trace $\langle tt\rangle$ is defined by (9), (10), and (15); $\hat{\delta}_2$ has still to be summed over the deuteron spin projections.

In order to perform the above integrations we decompose the nucleon-nucleon scattering amplitude t in terms of the partial waves summing over the total angular momentum J, the spin S of a two-particle state, and the angular momenta l and l' in the initial and final states:

$$\langle\mathbf{k}'S\nu'\mid t(E_{\mathrm{ef}})\mid\mathbf{k}S\nu\rangle=\sum_{Jll'}D^{JS}_{l'\nu'l\nu}(\hat{\mathbf{k}}',\hat{\mathbf{k}})T^{JS}_{l'l}(\mathbf{k}',\mathbf{k},E_{\mathrm{ef}}) \ . \tag{20}$$

Here

$$D^{JS}_{l'\nu'l\nu}(\hat{\mathbf{k}}'\hat{\mathbf{k}})=\sum_{M\mu\mu'}Y^{l'}_{\mu'}(\hat{\mathbf{k}}')Y^{l^*}_{\mu}(\hat{\mathbf{k}})\langle l'\mu'S\nu'\mid JM\rangle\langle JM\mid l\mu S\nu\rangle \tag{21}$$

is given by the spherical harmonics depending on the angles of the unit vectors $\hat{\mathbf{k}}'$ and $\hat{\mathbf{k}}$; M, ν, ν', μ, and μ' are the spin projections appearing in the Clebsch-Gordan coefficients. The partial wave amplitudes $T^{JS}_{l'l}(k',k,E_{\mathrm{ef}})$ are the functions of three variables: two momenta k and k' and the relative energy E_{ef}.

The scalar nucleon-nucleon amplitude t_s (3) can be written as

$$t_s(\mathbf{k}',\mathbf{k},E_{\mathrm{ef}})=\frac{1}{16\pi}\sum_{SJl}(2J+1)T^{JS}_{ll}(k',k,E_{\mathrm{ef}})P_l(\hat{\mathbf{k}}'\cdot\hat{\mathbf{k}}) \ . \tag{22}$$

Let us notice that only the diagonal elements in the angular momentum space l are present in Eq. (22) and P_l is the

Legendre polynomial which depends on the scattering angle θ between the vectors k and k'.

The trace $\langle tt \rangle$ in Eq. (19) reads

$$\langle tt \rangle = \frac{1}{4} \sum_{S\nu\nu_1} \sum_{Jl'l_1} \sum_{Ill_2} D^{JS}_{l'\nu l_1\nu_1}(\hat{\mathbf{k}}',\hat{\mathbf{k}}_1) D^{IS}_{l_2\nu_1 l\nu}(\hat{\mathbf{k}}_1,\hat{\mathbf{k}}) T^{JS}_{l'l_1}(k',k_1,E_{\rm ef}) T^{IS}_{l_2 l}(k_1,k,E_{\rm ef}) \ . \tag{23}$$

Writing this equation we have passed from the spin basis of two individual nucleons [in (15)] to the spin basis $S\nu$, without changing the trace value.

The next step in the evaluation of $\hat{\delta}_2$ (19) is the partial wave decomposition of two products:

$$\mathbf{Q}\cdot(\mathbf{k}'-\mathbf{k}_1)\mathbf{Q}\cdot(\mathbf{k}-\mathbf{k}_1) = 4\pi \sum_{\rho=0}^{2} \sum_{n=-\rho}^{\rho} Y^{\rho}_{m}(\hat{\mathbf{k}}_1)\cdot f_{\rho n}(\mathbf{Q},\mathbf{k},\mathbf{k}',k_1) \ , \tag{24}$$

where the functions $f_{\rho n}$ are defined as

$$f_{00}(\mathbf{Q},\mathbf{k},\mathbf{k}',k_1) = (\mathbf{Q}\cdot\mathbf{k}\mathbf{Q}\cdot\mathbf{k}' + \tfrac{1}{3}Q^2k_1^2) Y_0^0(\hat{\mathbf{Q}}) \ , \tag{25}$$

$$f_{1n}(\mathbf{Q},\mathbf{k},\mathbf{k}',k_1) = -\tfrac{2}{3}\mathbf{Q}\cdot\mathbf{u}Qk_1 Y_n^{1*}(\hat{\mathbf{Q}}) \ , \tag{26}$$

and

$$f_{2n}(\mathbf{Q},\mathbf{k},\mathbf{k}',k_1) = \tfrac{2}{15}Q^2k_1^2 Y_n^{2*}(\hat{\mathbf{Q}}) \ . \tag{27}$$

The vector $\mathbf{u}=(\mathbf{k}+\mathbf{k}')/2$ is perpendicular to the momentum transfer $\mathbf{q}$. In the following calculations we choose the z axis (spin-quantization axis) along $\mathbf{q}$ and the x axis along $\mathbf{u}$. Now we introduce the integrals

$$F_{\rho n} = \int d^3Q \ \psi^{\dagger}(\mathbf{Q}+\tfrac{1}{4}\mathbf{q}) f_{\rho n}(\mathbf{Q},\mathbf{k},\mathbf{k}',k_1) \psi(\mathbf{Q}-\tfrac{1}{4}\mathbf{q}) \tag{28}$$

which can be calculated in terms of the following functions already defined in Ref. 3:

$$G(\mathbf{a},\mathbf{b},\mathbf{q}) = \int d^3Q \ \psi^{\dagger}(\mathbf{Q}+\tfrac{1}{4}\mathbf{q})\mathbf{Q}\cdot\mathbf{a}\mathbf{Q}\cdot\mathbf{b}\psi(\mathbf{Q}-\tfrac{1}{4}\mathbf{q}) \ , \tag{29}$$

and

$$D(\mathbf{q}) = \int d^3Q \ \psi^{\dagger}(\mathbf{Q}+\tfrac{1}{4}\mathbf{q})Q^2\psi(\mathbf{Q}-\tfrac{1}{4}\mathbf{q}) \ . \tag{30}$$

In (29) $\mathbf{a}$ and $\mathbf{b}$ are arbitrary vectors and for the calculation of $F_{\rho n}$ it is convenient to use the standard spherical basis of unit vectors:

$$\mathbf{e}_{\pm 1} = \mp 1/\sqrt{2}(\mathbf{e}_x \pm i\mathbf{e}_y), \quad e_x = \mathbf{u}/u \ , \tag{31}$$

$$\mathbf{e}_0 = \mathbf{e}_z \equiv \mathbf{q}/q \ . \tag{32}$$

Then, for example,

$$Q Y_n^{1*}(\hat{\mathbf{Q}}) = (-1)^m \sqrt{3/4\pi}\,\mathbf{Q}\cdot\mathbf{e}_{-n}$$

and we can rewrite $F_{\rho n}$ in terms of the suitable combinations of $G(\mathbf{a},\mathbf{b},\mathbf{q})$ and $D(\mathbf{q})$. Next we average over the deuteron spin projections which means that we take only the *scalar* parts of the functions $F_{\rho n}$. In a few steps we get

$$(F_{00})_s = (4\pi)^{-1/2}(G_{0s} + \tfrac{1}{3}k_1^2 D_s) \ , \tag{33}$$

$$(F_{1n})_s = -(4\pi)^{-1/2}\sqrt{2/3}k_1 u \tfrac{1}{3}(D_s - C_s)n \ , \tag{34}$$

$$(F_{2n})_s = (4\pi)^{-1/2}\frac{2}{3\sqrt{5}}k_1^2 C_s \delta_{n0} \ , \tag{35}$$

where

$$G_{0s} = \tfrac{1}{3}[u^2(D_s - C_s) - \tfrac{1}{4}q^2(D_s + 2C_s)] \ , \tag{36}$$

C_S is the scalar part of the function (see Ref. 3)

$$C(\mathbf{q}) = \int d^3Q \ \psi(\mathbf{Q}+\tfrac{1}{4}\mathbf{q})Q^2 P_2(\hat{\mathbf{Q}}\cdot\hat{\mathbf{q}})\psi(\mathbf{Q}-\tfrac{1}{4}\mathbf{q}) \ , \tag{37}$$

and D_S is the scalar part of $D(\mathbf{q})$ given by (30). After the integration over the variable Q we come back to (19) where the integration over the angular part of $\mathbf{k}_1$ should be done. It can be made directly using the integration formulae[16] for the product of the three spherical harmonics [see (A1) in the Appendix]. As a result of splitting (24) into the different parts the full second-order correction δ_2 is also splitted:

$$\delta_2 = \delta_2(\rho=0) + \delta_2(\rho=1) + \delta_2(\rho=2) \ , \tag{38}$$

where

$$\delta_2(\rho=0) = \tfrac{1}{3}D_S(q)\frac{1}{m}\frac{dt_s(\mathbf{k}',\mathbf{k},E_{\rm ef})}{dE_{\rm ef}} + \frac{1}{48\pi m^2}[u^2(2D_S - C_S) - \tfrac{1}{2}q^2 C_S] \sum_{l=0}^{\infty} P_l(\hat{\mathbf{k}}\cdot\hat{\mathbf{k}}') \int_0^{\infty} dk_1 k_1^2 \frac{\sum_{SJl_1}(2J+1)[T^{JS}_{ll_1}(k,k_1,E_{\rm ef})]^2}{(E_{\rm ef} - k_1^2/m)^3} \ , \tag{39}$$

$$\delta_2(\rho=1) = \frac{1}{6}\frac{u\sqrt{2}}{m^2}(D_S - C_S) \sum_{l'l\mu} \mathrm{Re}[Y^{l'}_{1+\mu}(\hat{\mathbf{k}}')Y^{l}_{-\mu}(\hat{\mathbf{k}})] \int_0^{\infty} dk_1 k_1^3 \frac{F_{ll'\mu}(k_1)}{(E_{\rm ef} - k_1^2/m)^3} \ , \tag{40}$$

and

$$\delta_2(\rho=2) = \frac{1}{6}\frac{C_S(q)}{m^2} \sum_{l'l\mu} Y^{l'}_{\mu}(\hat{\mathbf{k}}')Y^{l}_{-\mu}(\hat{\mathbf{k}}) \int_0^{\infty} dk_1 k_1^4 \frac{G_{ll'\mu}(k_1)}{(E_{\rm ef} - k_1^2/m)^3} \ . \tag{41}$$

The expressions for the integrands $F_{ll'\mu}$ and $G_{ll'\mu}$ are rather long and their derivation is given in the Appendix. In (36) we have the energy derivative $dt_s/dE_{\rm ef}$ which can be directly calculated or related to the following integral expression [compare (32) of Ref. 3]

$$\frac{dt_s(\mathbf{k}',\mathbf{k},E_{\rm ef})}{dE_{\rm ef}}=-\frac{1}{16\pi}\sum_{SJl}(2J+1)P_l(\hat{\mathbf{k}}\cdot\hat{\mathbf{k}}')\sum_{l_1}\int_0^\infty dk_1 k_1^2\frac{[T_{ll_1}^{JS}(k,k_1,E_{\rm ef})]^2}{(E_{\rm ef}-k_1^2/m)^2}\ . \tag{42}$$

Let us remark that the term $\delta_2(\rho=0)$ is the most important term, as one can see from (24)–(27), the part $\delta_2(\rho=1)$ vanishes for the backward scattering ($u=0$) and the correction $\delta_2(\rho=2)$ vanishes for the forward scattering [$C_S(q=0)=0$, Eq. (37)].

IV. NUCLEON-NUCLEON AMPLITUDES AND THEIR ENERGY DERIVATIVE

In (39) and (42) we meet the partial derivative over the effective energy of the nucleon-nucleon scattering amplitude. We stress here that during the calculation of this quantity we *fix* the incoming and outgoing relative momenta $\mathbf{k}$ and $\mathbf{k}'$, so we are dealing with *off-shell* amplitudes. The energy dependence of this derivative as well as the nucleon-nucleon amplitude itself is important in the study of the $\delta_2(\rho=0)$ correction. In Ref. 3 $dt/dE_{\rm ef}$ was parametrized as

$$\frac{dt_s}{dE_{\rm ef}}=\alpha E_{\rm ef}^{-1}t_s\ , \tag{43}$$

where α was a parameter. Two values of this parameter has been considered: $\alpha=-1$, and $\alpha=+1$. Now we can calculate exactly $dt/dE_{\rm ef}$. The calculations have been done numerically for the three realistic nucleon-nucleon potentials as indicated in the Introduction. We discuss two cases: the proton scattering on the target neutron and the proton scattering on the proton bound in the deuteron neglecting the Coulomb part of the realistic interaction.

Let us define the complex function (which we also call α) of the energy $E_{\rm ef}$ and the scattering angle θ_N (in the *nucleon-nucleon* center of mass system)

$$\alpha=\frac{E_{\rm ef}}{t_s}\frac{dt_s}{dE_{\rm ef}}\ . \tag{44}$$

In Figs. 1 and 2 we show the laboratory energy $E_{\rm lab}$ dependence of the real part of α for the *pn* and *pp* scattering, respectively, and in Figs. 3 and 4 the imaginary part of α for the two angles $\theta_N=0°$ and 180°. The real part of α is related to the behavior of the amplitude modulus and the imaginary part of α to its phase ϕ:

$$\mathrm{Re}\alpha=\frac{E_{\rm ef}}{|t_s|}\frac{d|t_s|}{dE_{\rm ef}}\ , \tag{45}$$

$$\mathrm{Im}\alpha=E_{\rm ef}\frac{d\phi}{dE_{\rm ef}}\ . \tag{46}$$

Since we use the nonrelativistic kinematics the effective *laboratory* kinetic energy $E_{\rm lab}$ is twice as large as the center of mass energy $E_{\rm ef}$ [the formulae for $E_{\rm ef}$ are in Ref. 3, Eqs. (21) and (46)]. In Figs. 1–4 we notice the substantial dependence of α on the energy, the scattering angle, and the type of the potential. One common feature of α is that both the real and imaginary parts remain relatively *small in comparison with 1*. It means that the so-called time delay[8] in the nucleon-nucleon interactions at these energies is small (of the order of 0.5 fm/c or less where c is the light velocity).

In Figs. 5 and 6 we plot the modulus of α. For the proton-neutron scattering at about 150 MeV it is smaller than about 0.2 for the forward and backward scattering and then gradually grows with energy. For the proton-proton case at 0° $|\alpha|$ increases with energy while for the backward scattering it firstly decreases, has a minimum at about 325 MeV and then slightly increases. In general $|\alpha|$ is larger for the *pp* scattering than for the *pn* scattering.

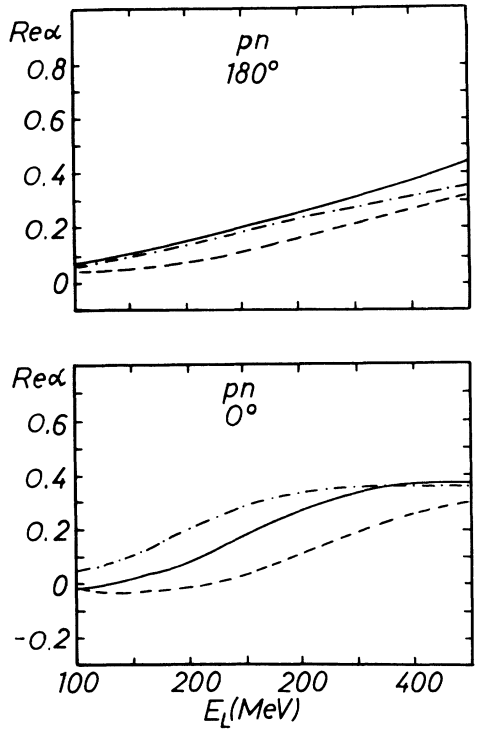

FIG. 1. Real part of the parameter α defined by (44) as a function of the effective laboratory kinetic energy for the scattering angles 0° and 180° in the *pn* c.m. system. The solid line corresponds to the Argonne potential, the dashed line to the SSCC potential, and the dashed-dotted line to RSC potential.

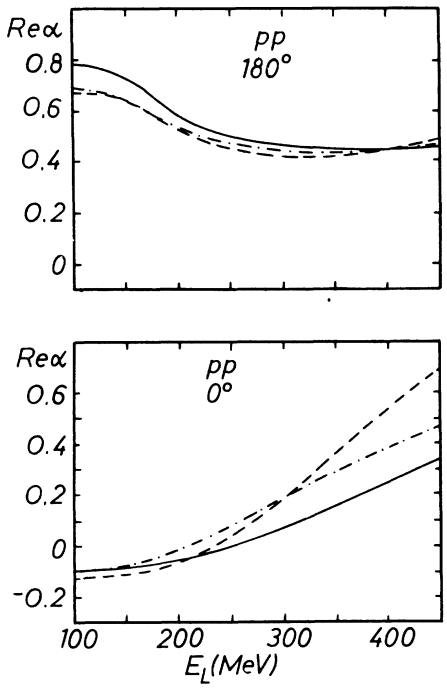

FIG. 2. Same as Fig. 1 but for the *pp* scattering.

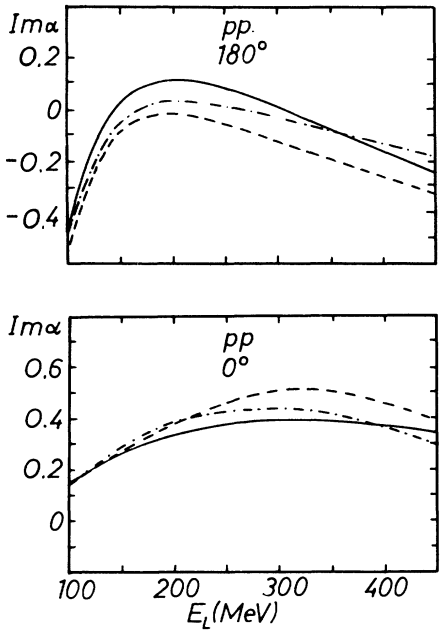

FIG. 4. Same as Fig. 3 but for the *pp* scattering.

The angular dependence of α also varies with energy, type of the target particle and the potential. As a general rule the energy derivative is more sensitive to the type of potential than the scattering amplitude itself because the latter has been constructed to reproduce the known nucleon-nucleon scattering data or the experimentally found phase shifts. The moduli of the nucleon-nucleon scalar amplitudes t_s in the region of our interest have the maxima at 0° (forward diffraction peak) and 180° (the backward peak, due to the existence of exchange forces). In some cases the backward peak is even more pronounced than the forward one. In general we observe a more rich angular structure in t_s and dt_s/dE at higher energies. This is due to the interference of higher partial waves which become important only at high enough energies. In the preceding calculations we have summed over all the partial waves up to $J=7$, the maximum l value was 6. For $l \geq l_{\max}$ we have added the one-pion-exchange

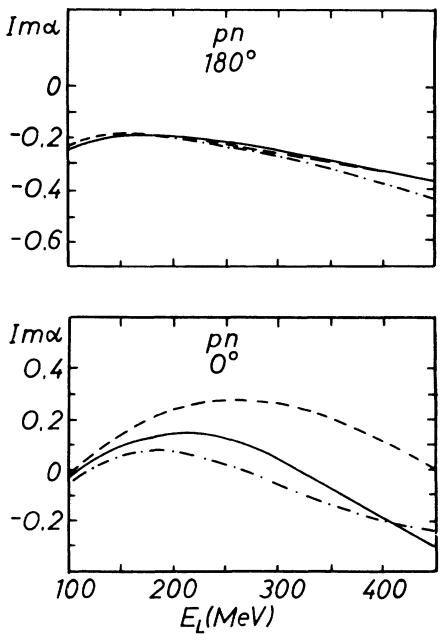

FIG. 3. Imaginary part of the parameter α. See Fig. 1 caption.

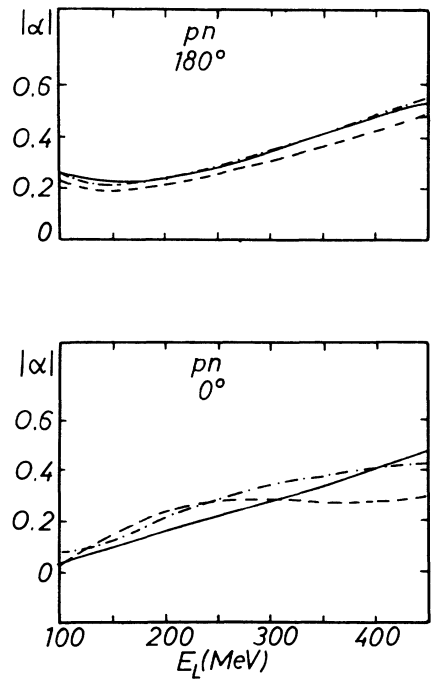

FIG. 5. Modulus of the parameter α. See Fig. 1 caption.

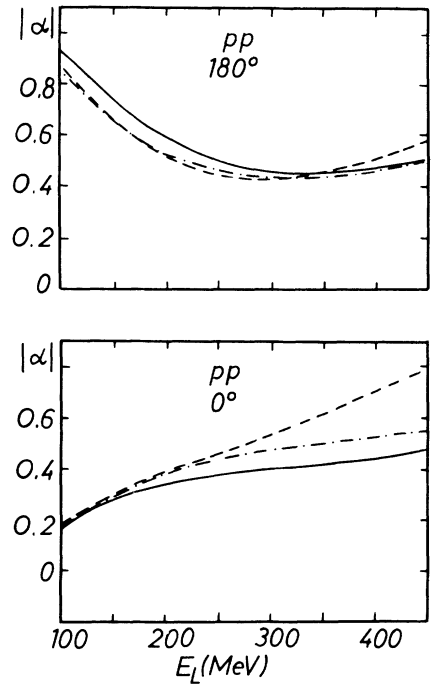

FIG. 6. Same as Fig. 5 but for the *pp* scattering.

amplitude calculated as in Ref. 9. The results shown in Figs. 7–17 have been obtained for $l_{\max}=8$. We have checked that the differences between $l_{\max}=6$ and $l_{\max}=8$ or 10 are at most a few percent of the $|\alpha|$ values.

In Fig. 7 we give the example of the t_s and dt_s/dE_L variation as a function of the scattering angle and in Fig.

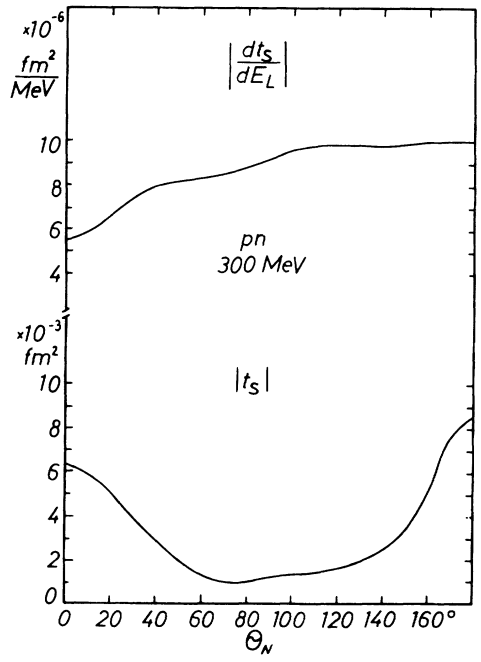

FIG. 7. Angular dependence of the modulus of the scalar *pn* scattering amplitude and its energy derivative calculated at 300 MeV for the Argonne potential.

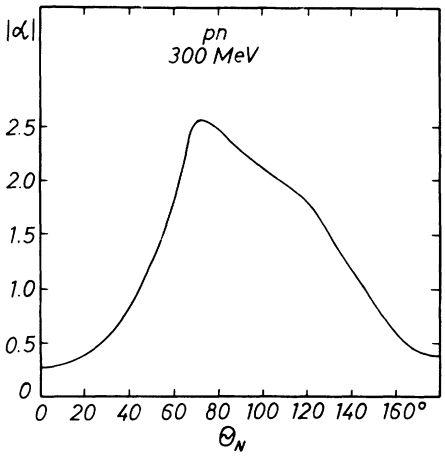

FIG. 8. Angular dependence of the α modulus. See Fig. 7 caption.

8 we give the corresponding $|\alpha|$ plot. We see that $|\alpha|$ has the maximum values at the angles close to 90° which is the natural reflection of the minimum of $|t|$. We therefore pay a special attention to this angle during the discussion of the second-order correction values.

V. NUMERICAL RESULTS AND DISCUSSION

We stress the fact that the results depend on the *effective* laboratory energy $E_{\rm lab}$ which is an increasing function of the scattering angle. For example the laboratory effective energy $E_{\rm lab}=450$ MeV at 180° corresponds to the beam laboratory energy of 253 MeV only.

We wish to evaluate the second-order correction terms given by (38)–(41) in comparison to the "optimal" amplitude (2). Therefore, we introduce the relative correction β

$$\beta=\left|\frac{\delta_2}{T_s}\right| . \tag{47}$$

The value of T_s is proportional to the scalar deuteron form factor ϕ_S which is plotted in Fig. 9 as a function of the momentum transfer q. The region of the momentum transfer which is a subject of our interest in this paper is limited to the value about 4.7 fm^{-1} which is related to the maximum energy 450 MeV for the backward scattering. It roughly corresponds to the zero of the scalar form factor. The other deuteron functions $D_S(q)$ and $C_S(q)$ are plotted in Figs. 10 and 11. They have the values measured in fm^{-2} and enter in some linear combinations as seen in (39) and (40). The function $C_S(q)$ is, however, much smaller than the corresponding function $D_S(q)$. In the region of q up to 4.7 fm^{-1} the *maximum* values $|C_S/D_S|$ are 5.5%, 8%, and 10% for the RSC, Argonne, and SSCC potentials, respectively. By inspection in the structure of (38)–(41) we notice that the $\delta_2(\rho=2)$ is very small in comparison with $\delta_2(\rho=0)$ and therefore we neglect it. Since our main interest lies in the relatively large momentum transfer range we can also neglect the $\delta_2(\rho=1)$ correction which vanishes for the backward

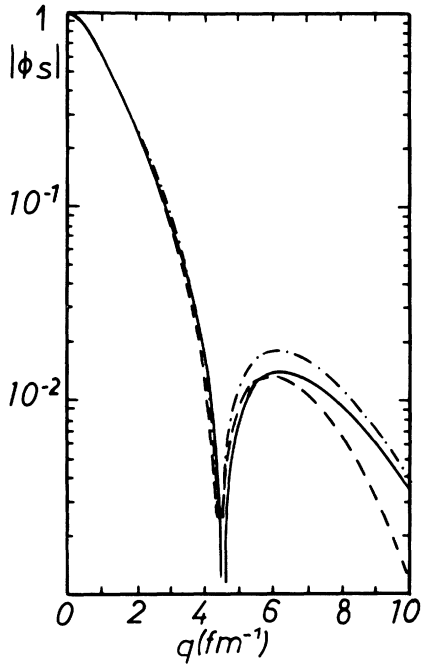

FIG. 9. The deuteron scalar form factor as a function of the momentum transfer. See Fig. 1 caption.

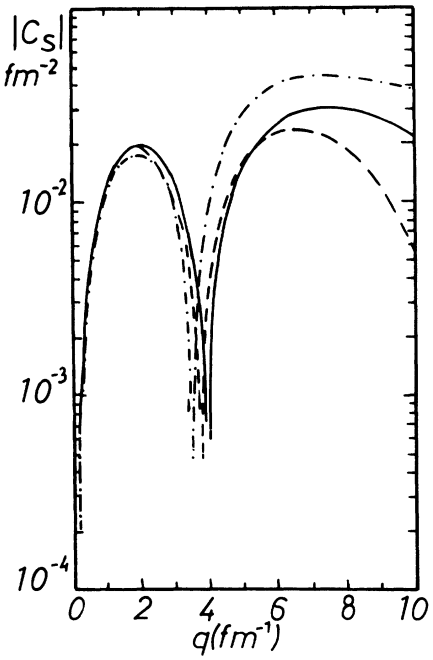

FIG. 11. Momentum transfer dependence of the scalar part of the function C defined in (37). See Fig. 1 caption.

scattering at any energy. Next we observe that at 180° the second term of $\delta_2(\rho=0)$ is proportional to $C_S(q)$ (because $u=0$ here) and therefore, for the backward scattering we get a very simple approximated result

$$\delta_s \approx \tfrac{1}{3} D_S(q) \frac{1}{m} \frac{dt_s}{dE_{\rm ef}} \ . \tag{48}$$

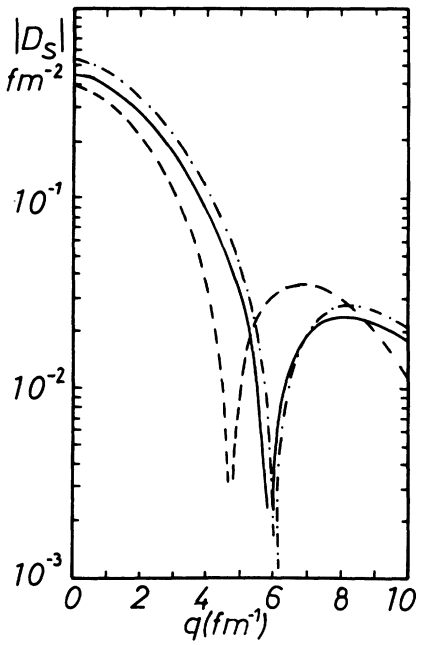

FIG. 10. Momentum transfer dependence of the scalar part of the function D defined in (30). See Fig. 1 caption.

Using (44) this correction can be written as

$$\delta_2 = \tfrac{1}{3} \alpha \frac{D_S(q)}{m E_{\rm ef}} t_s \ . \tag{49}$$

Let us remark that if $\alpha=-1$ we get exactly (40) of Ref. 3, the only difference is that now α is not a fixed parameter but the calculable function of the angle and the energy. The approximation (48) amounts to 85% or even 100% of the whole δ_2 contribution for the backward scattering angles $\theta \gtrsim 90°$ (θ is defined in the proton-*deuteron* center of mass system) provided we treat the range of q where $C_S(q)/D_S(q)$ remains small. In our case this covers all the energy range for the Reid-Day and Argonne potentials and up to about 380 MeV for the SSCC potential. For the latter case the functions $|D_S(q)|$ and $|C_S(q)|$ have the similar values starting from $q \approx 4.3$ fm^{-1}.

The relative correction β, valid for the large scattering angles where δ_2 can be approximated by (49), is

$$\beta \approx \tfrac{1}{3} |\alpha| \frac{|D_S(q)|}{m E_{\rm ef} |\phi_S(q)|} \ . \tag{50}$$

From this formula one can easily estimate the order of magnitude of β knowing $|\alpha|$ (from Sec. IV) and the ratio D_S/ϕ_S. It becomes relatively small and *stable* at 180° up to $E_{\rm lab} \approx 330$ MeV both for the proton-neutron and proton-proton interactions. The factor $E_{\rm ef}^{-1}$ in (49) is balanced by the increasing ratio D_S/ϕ_S and increasing modulus of α for larger energies (especially for the *pn* case). The energy dependence of β calculated using the *complete* $\delta_2(\rho=0)$ term is shown in Figs. 12 and 13 where the sensitivity of the results to the form of the chosen potential is exhibited. The corrections are of the order of 10–20 %. We should mention, however, that at about

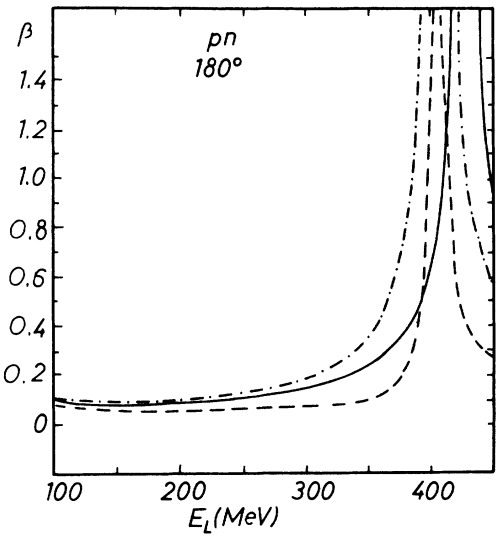

FIG. 12. Energy dependence of the relative second-order correction (47) for the *pn* scattering at 180°.

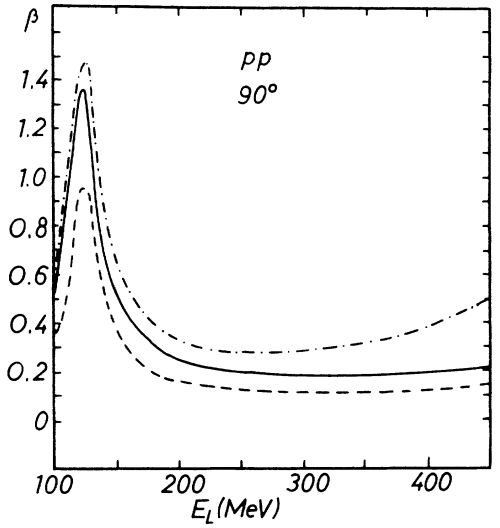

FIG. 14. Relative second-order correction as a function of energy for the *pp* scattering at 90° in the *p-d* center of mass system.

400 MeV there is a region where the relative corrections β become large. The reason of this behavior is the vicinity of the zero of the scalar deuteron form factor ϕ_S to which is the proportional the "optimal" amplitude (2). Similar situation, where the "optimal" approximation is not valid, exists in the case of very small value of the modulus of the proton-target nucleon amplitude $|t_s|$. An example of such a situation is illustrated in Fig. 14. We see the clear peak at the energy of about 125 MeV and $\theta=90°$ for the proton-proton scattering. The origin of this maximum is that both the real and imaginary parts of t_s go through zero at the close (but not identical) angles. From Fig. 14 and especially from Fig. 15 we can notice the larger values of the corrections β at 90° than at 180°. The primary reason of this dependence is the smaller value of $|t_s|$ at 90°.

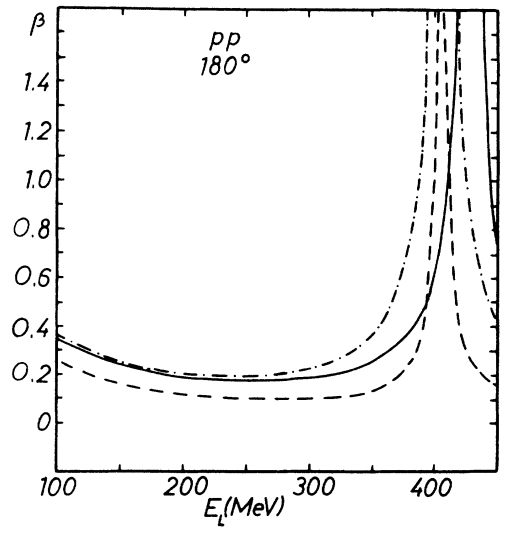

FIG. 13. Same as Fig. 12 but for the *pp* scattering.

The correction β in the forward direction is given in Fig. 16. It is extremely small (1–2 %) for the *pp* case and stays within about 5% for the *pn* case. Its smallness confirms once again the fact that the impulse approximation which is equivalent to the "optimal" approximation for this particular angle is a good approximation of the full amplitude.

For completeness we show in Fig. 17 the full angular dependence of β for $E_{\text{lab}}=300$ MeV. The smallest values of β are in the forward and backward directions where the nucleon-nucleon amplitude moduli have the maxima.

VI. SUMMARY AND CONCLUSIONS

We have calculated the first- and second-order corrections to the elastic proton scattering on the proton or

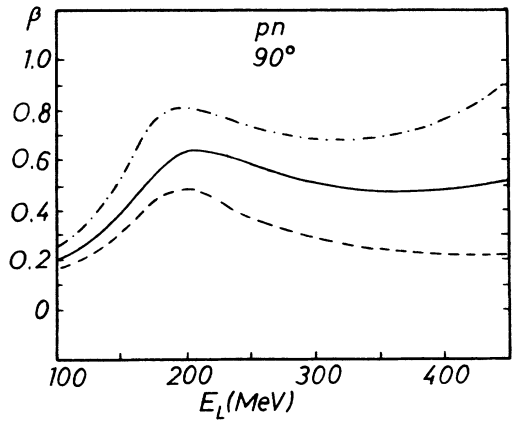

FIG. 15. Same as Fig. 14 but for the *pn* scattering.

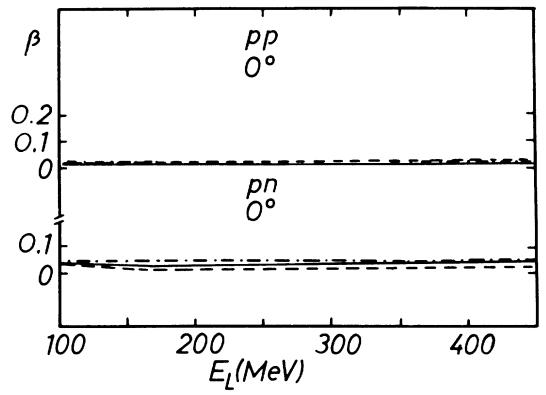

FIG. 16. Same as Figs. 14 and 15 but for the forward scattering.

neutron bound in deuterium. Three types of realistic nucleon-nucleon interactions have been applied. The laboratory energy has been varied between 100 and 450 MeV and the full range of the scattering angles has been covered. The special emphasis has been put on the large-angle scattering. We have evaluated the relative correction to the "optimal" amplitude averaged over the proton and deuteron initial and final spin projections. In the forward direction this correction is of the order of 1–5% and does not vary rapidly with energy. For the backward scattering up to energy of about 320 MeV the *pn* corrections are smaller than the *pp* ones both being of the order of 10–20%. In the vicinity of 400 MeV they become very large because this energy corresponds to the zero of the deuteron scalar form factor. In this region the "optimal" approximation cannot be applied. The magnitude of the corrections seems to be related to the hardness of the core of the realistic potential and in the same manner to the percentage of the deuteron *D* state wave function. The smallest corrections are for the super-soft-core potential, the largest one for the Reid-Day potential. The Argonne potential leads to the intermediate values between the above potentials.

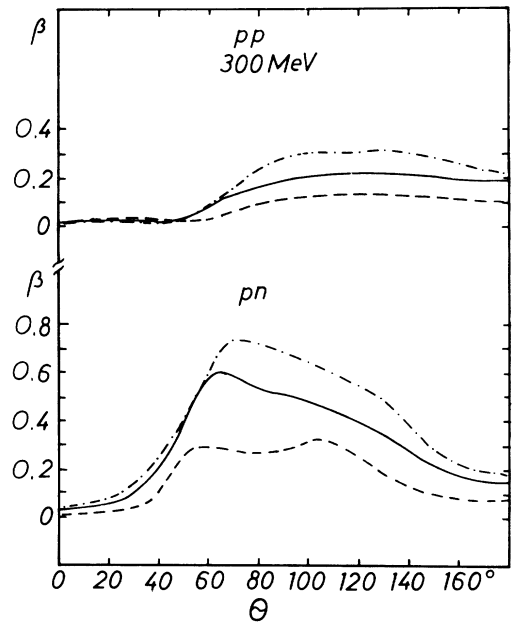

FIG. 17. Angular dependence of the second-order relative correction for the *pp* and *pn* scattering at 300 MeV. See Fig. 1 for description of lines.

The relative correction can be comparatively large for the scattering angles close to 90° as Fig. 15 indicates for the *pn* scattering. In some cases the dip in the modulus of the nucleon-nucleon amplitude can enforce the relative ratio of the corrections as it is seen in Fig. 14 for the *pp* scattering at about 125 MeV. This fact illustrates the necessity of a careful application of the "optimal" approximation in the kinematical situation where the single scattering amplitude is small or goes through zero. In this energy region the most important relative corrections are present at the angles close to 90°, the presence of the backward peak of the nucleon-nucleon amplitude modulus diminishes the relative correction values.

At the end we would like to make the following remark on the eventual extrapolation of the energy dependence of the relative corrections at the backward scattering angles. We have already seen that it is a rather complicated function of energy. At lower energies between about 100 and 200 MeV it has a tendency of decreasing especially visible in Fig. 13 for the *pp* case. We cannot, however, say that after the peak at about 400 MeV the corrections will decrease in a monotonic way. First of all, as mentioned in Ref. 3, the ratio D_S/ϕ_S continue to increase with energy at the fixed angle. The second point is that the coefficient $|\alpha|$, related to energy derivative of the nucleon-nucleon amplitude, has a slight tendency to increase with increasing energy (more clear for the *pn* case), so the correction β does not behave like $E_{\rm ef}^{-1}$. The present approach of using the realistic potentials to calculate the nucleon-nucleon amplitudes is no longer possible for the energies larger than about 450 MeV because the pion production processes become important and the potential formalism cannot be applied without a substantial modification. We can, however, expect an increase of the energy derivative of the scalar nucleon-nucleon amplitude because the latter is closely related via the optical theorem to the increasing total cross section for the nucleon-nucleon interaction. Testing the validity of the "optimal" approximation in the higher-energy region remains an open problem.

As the final remark we would like to point out that the present test of the *pd* single scattering amplitude in the "optimal" approximation can be easily extended to the elastic nucleon scattering on the complex nuclei. The structure of the first-order optical potential in this approximation is the same as considered above for the *pd* single scattering amplitude (see Ref. 2). The main difficulty lies in a rather poor knowledge of the high momentum components of the heavy nucleus wave function which fortunately has not been the case in the present analysis done for the deuterium target.

ACKNOWLEDGMENTS

One of us (L.L.) would like to thank Dr. S. A. Gurvitz, Dr. B. Loiseau, and Dr. W. Plessas for interesting discussions and Dr. M. Różańska for help in the numerical calculations. The Division de Physique Théorique is associated with Centre National de la Recherche Scientifique (CNRS).

APPENDIX

The direct step to get the formulae for the functions $F_{ll'\mu}(k_1)$ and $G_{ll'\mu}(k_1)$ appearing in (40) and (41) is the following integration formula over the angles of the $\hat{\mathbf{k}}_1$ vector:

$$\int d\hat{\mathbf{k}}_1 Y^{\rho}_{m}(\hat{\mathbf{k}}_1) D^{JS}_{l'\nu l_1\nu_1}(\hat{\mathbf{k}}',\hat{\mathbf{k}}_1) D^{IS}_{l_2\nu_1 l\nu}(\hat{\mathbf{k}}_1,\hat{\mathbf{k}})$$

$$= (2J+1)(2I+1)(4\pi)^{-1/2}[(2\rho+1)(2l_1+1)(2l_2+1)]^{1/2}(-1)^{l_1+l_2+l+l'+m+\nu-\nu_1}$$

$$\times \begin{pmatrix} \rho & l_1 & l_2 \\ 0 & 0 & 0 \end{pmatrix} \sum_{\mu} Y^{l'}_{m+\mu}(\hat{\mathbf{k}}') Y^{l}_{-\mu}(\hat{\mathbf{k}}) \begin{pmatrix} l' & S & J \\ m+\mu & \nu & -m-\nu-\mu \end{pmatrix} \begin{pmatrix} l & S & I \\ \mu & \nu & -\mu-\nu \end{pmatrix}$$

$$\times \begin{pmatrix} l_1 & S & J \\ m+\nu-\nu_1+\mu & \nu_1 & -m-\mu-\nu \end{pmatrix} \begin{pmatrix} l_2 & S & I \\ \mu+\nu-\nu_1 & \nu_1 & -\mu-\nu \end{pmatrix} \begin{pmatrix} \rho & l_1 & l_2 \\ m & -m-\mu-\nu+\nu_1 & \mu+\nu-\nu_1 \end{pmatrix} . \tag{A1}$$

For $\rho=0$ further simplifications are possible which after a suitable rearrangement of the factor $k_1^4(E_{\rm ef}-k_1^2/m)^{-3}$ lead directly to (39). For $\rho=1$ and $\rho=2$ the formulae are given below:

$$F_{ll'\mu}(k_1)=\sum_{SJIl_1l_2}(2J+1)(2I+1)[(2l_1+1)(2l_2+1)]^{1/2}\begin{pmatrix} 1 & l_1 & l_2 \\ 0 & 0 & 0 \end{pmatrix} V^{JIS\mu}_{l'l_1l_2l} T^{JS}_{l'l_1}(k',k_1,E_{\rm ef}) T^{IS}_{l_2l}(k_1,k,E_{\rm ef}) , \tag{A2}$$

where

$$V^{JIS\mu}_{l'l_1l_2l}=\sum_{\nu\nu_1}(-1)^{\nu-\nu_1}\begin{pmatrix} 1 & l_1 & l_2 \\ 1 & -1-\mu-\nu+\nu_1 & \mu+\nu-\nu_1 \end{pmatrix}\begin{pmatrix} l' & S & J \\ 1+\mu & \nu & -1-\mu-\nu \end{pmatrix}$$

$$\times \begin{pmatrix} l_1 & S & J \\ 1+\nu-\nu_1+\mu & \nu_1 & -1-\nu-\mu \end{pmatrix}\begin{pmatrix} l_2 & S & I \\ \mu+\nu-\nu_1 & \nu_1 & -\mu-\nu \end{pmatrix}\begin{pmatrix} l & S & I \\ \mu & \nu & -\mu-\nu \end{pmatrix} \tag{A3}$$

and

$$G_{ll'\mu}(k_1)=\sum_{SJIl_1l_2}(2J+1)(2I+1)[(2l_1+1)(2l_2+1)]^{1/2}\begin{pmatrix} 2 & l_1 & l_2 \\ 0 & 0 & 0 \end{pmatrix} W^{JIS\mu}_{l'l_1l_2l} T^{JS}_{l'l_1}(k',k_1,E_{\rm ef}) T^{IS}_{l_2l}(k_1,k,E_{\rm ef}) ,$$

where

$$W^{JIS\mu}_{l'l_1l_2l}=\sum_{\nu\nu_1}(-1)^{\nu-\nu_1}\begin{pmatrix} l_1 & l_2 & 2 \\ -\mu-\nu+\nu_1 & \mu+\nu-\nu_1 & 0 \end{pmatrix}\begin{pmatrix} l' & S & J \\ \mu & \nu & -\mu-\nu \end{pmatrix}$$

$$\times \begin{pmatrix} l_1 & S & J \\ \nu-\nu_1+\mu & \nu_1 & -\mu-\nu \end{pmatrix}\begin{pmatrix} l & S & I \\ \mu & \nu & -\mu-\nu \end{pmatrix}\begin{pmatrix} l_2 & S & I \\ \nu-\nu_1+\mu & \nu_1 & -\mu-\nu \end{pmatrix} . \tag{A4}$$

In (A1), (A2), and (A3) we used the symmetry relations of $3j$ symbols and the spherical harmonics to relate $n=-1$ term (34) with $n=1$ term.

[1] S. A. Gurvitz, J.-P. Dedonder, and R. D. Amado, Phys. Rev. C **19**, 142 (1979).

[2] S. A. Gurvitz, Phys. Rev. C **33**, 422 (1986).

[3] L. Leśniak, Nucl. Phys. **A403**, 589 (1983).

[4] Y. Koike, J. Haidenbauer, and W. Plessas, Phys. Rev. C **35**, 396 (1987).

[5] J. L. Ballot, M. l'Huilllier, and P. Benoist-Gueutal, Phys. Rev. C **12**, 725 (1975).

[6] R. L. Workman and H. W. Fearing, Phys. Rev. C **34**, 780 (1986).

[7] E. F. Redish and K. Stricker-Bauer, Phys. Rev. C **36**, 513 (1987).

[8]M. L. Goldberger and K. M. Watson, *Collision Theory* (Wiley, New York, 1964).
[9]R. V. Reid, Jr., Ann. Phys. (N.Y.) **50**, 411 (1968).
[10]B. D. Day, Phys. Rev. C **24**, 1203 (1981).
[11]R. de Tourreil and D. W. L. Sprung, Nucl. Phys. **A201**, 193 (1973).
[12]R. B. Wiringa, R. A. Smith, and T. L. Ainsworth, Phys. Rev. C **29**, 1207 (1984).
[13]S. A. Gurvitz, Phys. Rev. C **22**, 725 (1980).
[14]G. Alberi, M. Błeszyński, and T. Jaroszewicz, Ann. Phys. (N.Y.) **142**, 299 (1982).
[15]R. Oehme, Phys. Rev. **98**, 216 (1955).
[16]A. R. Edmonds, *Angular Momentum in Quantum Mechanics* (Princeton University Press, Princeton, New Jersey, 1957).